PROCEEDINGS OF SCIENCE

# Study of $e^+e^-$ annihilation into hadrons with the SND detector at the VEPP-2000 collider

**M. N. Achasov[ab], A. Yu. Barnyakov[ab], K. I. Beloborodov[ab], A. V. Berdyugin[ab], A. G. Bogdanchikov[a], A. A. Botov[a], T. V. Dimova[ab], V. P. Druzhinin*[ab], V. B. Golubev[ab], L. V. Kardapoltsev[ab], A. G. Kharlamov[ab], A. A. Korol[ab], S. V. Koshuba[a], D. P. Kovrizhin[ab], A. S. Kupich[a], K. A. Martin[ab], A. E. Obrazovsky[a], E. V. Pakhtusova[a], S. I. Serednyakov[ab], D. A. Shtol[ab], Z. K. Silagadze[ab], I. K. Surin[ab], Yu. V. Usov[ab] and A. V. Vasiljev[ab]**

[a] *Budker Institute of Nuclear Physics, Novosibirsk, 630090, Russia*
[b] *Novosibirsk State University, Novosibirsk, 630090, Russia*
*E-mail:* druzhinin@inp.nsk.su

Beginning from 2010, experiments with the SND detector are carrying out at the $e^+e^-$ collider VEPP-2000 in the energy range 0.3–2.0 GeV. The new results on study of the processes of $e^+e^-$ annihilation into hadrons are presented.

*The European Physical Society Conference on High Energy Physics*
*22–29 July 2015*
*Vienna, Austria*

*Speaker.





PoS(EPS-HEP2015)512

## 1. Detector and experiment

The SND [1, 2, 3, 4] is the general purpose nonmagnetic detector collecting data at the $e^+e^-$ collider VEPP-2000 [5]. Its main part is a spherical three-layer electromagnetic calorimeter containing 1640 NaI(Tl) crystals. The calorimeter covers a solid angle of 90% of $4\pi$. Directions of charged particles are measured by a tracking system based on a nine-layer drift chamber and one-layer proportional chamber with cathode strip readout. The particle identification is provided by $dE/dx$ measurements in the tracking system and a system of aerogel Cherenkov counters. Outside the calorimeter a muon detector consisting of proportional tubes and scintillation counters is located.

Experiments with the SND detector at the VEPP-2000 collider were carried out in 2010-2013. The total integrated luminosity collected in the center-of-mass (c.m.) energy range 0.32–2.00 GeV is 69 pb$^{-1}$ (47 pb$^{-1}$ above 1.05 GeV). Currently the VEPP-2000 accelerator complex is under upgrade. Experiments with increased luminosity are expected to be started in 2016.

The physics program of the VEPP-2000 experiments includes the following main topics:

- Measurement of exclusive hadronic cross sections below 2 GeV. The goal is to obtain the total cross section for $e^+e^- \to$ hadrons, which is used for calculation hadronic vacuum-polarization contribution to the muon $(g-2)$ and the running $\alpha_{QED}$.
- Study of dynamics of hadron production, i.e. separation between different intermediate states, for example, $\omega\eta$, $\phi\eta$, $\rho a_0$, etc. in the reaction $e^+e^- \to \pi^+\pi^-\pi^0\eta$. This is needed for understanding hadronization mechanisms.
- Hadron spectroscopy: study of light-vector-meson excitations, in particular, search for their radiative decays.
- Search for rare and forbidden decays of the $\rho$, $\omega$ and $\phi$ mesons.
- Study of nucleon-antinucleon pair production, extraction of the proton and neutron electromagnetic form factors.
- Two-photon physics, in particular, measurement of the photon-meson transition form factors for $\pi^0$, $\eta$, $\eta'$.
- Search for production of $C$-even resonances: $e^+e^- \to \eta$, $\eta'$, $f_1$, $f_2$, $a_2$ ...
- Using radiative return technique as alternative method for measurement of hadronic cross sections.

In this paper we present results of analysis of SND data collected in 2010-2013.

## 2. Hadronic cross sections

The process $e^+e^- \to \pi^+\pi^-\pi^0$ has been studied by SND above 1.05 GeV [6]. The measured cross section is shown in Fig. 1 in comparison with previous measurements. Our results are in agreement with the SND measurements at VEPP-2M and the BABAR data, but disagree with DM2. This is the most precise measurement to date. The two maxima in the cross section correspond to the $\omega(1420)$ and $\omega(1650)$ resonances. Their amplitudes interfere with the tails of $\omega(782)$ and $\phi(1020)$ resonances, and with each other. The $e^+e^- \to \pi^+\pi^-\pi^0$ reaction is the only process, in which the $\omega(1420)$ resonance is clearly seen. Above 1.8 GeV the cross-section energy dependence

cannot be described by contributions of known resonances. The nonresonant term has been added into the fitting function to obtain acceptable $P(\chi^2)$ for the fit shown in Fig. 1.

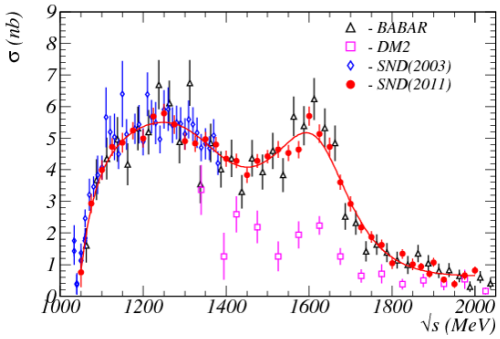


**Figure 1:** The $e^+e^- \to \pi^+\pi^-\pi^0$ cross section measured by SND at VEPP-2000 [SND(2011)] in comparison with previous measurements. The curve is the result of the fit with the $\omega(782)$, $\phi(1020)$, $\omega(1420)$, and $\omega(1650)$ resonances, and a nonresonant term needed to describe data above 1.8 GeV.

The $e^+e^- \to \eta\pi^+\pi^-$ process has been studied in the $\eta \to \gamma\gamma$ decay mode [7]. It is usually assumed that the dominant mechanism for this process is $\rho(770)\eta$. We observe the difference between the data $\pi^+\pi^-$ mass spectrum and the spectrum for simulation in the $\rho(770)\eta$ model [see Fig. 2(left)], which indicates a contribution of other mechanism, presumably $\rho(1450)\eta$. The measured $e^+e^- \to \eta\pi^+\pi^-$ cross section is shown in Fig. 2(right). Our result agrees with the BABAR measurement, but has better accuracy. The solid curve in Fig. 2(right) shows the result of the fits using the vector-meson-dominance (VMD) model with the $\rho(770)$, $\rho(1450)$ and $\rho(1700)$ resonances. The dashed curve represents the same model but without the $\rho(1700)$ contribution. It is seen that the $\rho(1450)$ resonance gives a dominant contribution into the $e^+e^- \to \eta\pi^+\pi^-$ cross section.

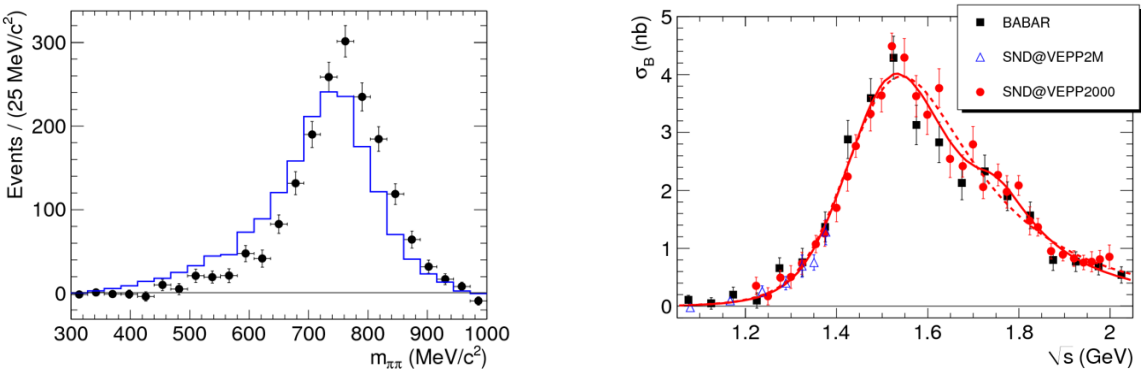


**Figure 2:** Left: The $\pi^+\pi^-$ invariant-mass spectra for data (points with error bars) and simulated (histogram) $e^+e^- \to \eta\pi^+\pi^-$ events. The simulation uses a model of the $\eta\rho(770)$ intermediate state. Right: The $e^+e^- \to \eta\pi^+\pi^-$ cross section measured by SND at VEPP-2000 (SND@VEPP2000) and in previous experiments. The solid curve is the result of the VMD fit with the $\rho(770)$, $\rho(1450)$ and $\rho(1700)$ resonances. The dashed curve is the same fit without the $\rho(1700)$ contribution.

From the fit we determine the product $B(\rho(1450) \to e^+e^-)B(\rho(1450) \to \eta\pi^+\pi^-) = (4.3 \pm 1.1) \times 10^{-7}$. Using $\rho(1450)$ measurements in other decay modes we extract the ratio $B(\rho(1450) \to$

$\omega\pi) : B(\rho(1450) \to \eta\pi^+\pi^-) : B(\rho(1450) \to \pi^+\pi^-) = (12.3 \pm 3.1) : 1 : (1.3 \pm 0.4)$, which can be compared with predictions $(7-8) : 1 : (4-10)$ [8, 9]. The CVC hypothesis has been used to calculate $B_{CVC}(\tau^- \to \eta\pi^-\pi^0\nu_\tau) = (0.156 \pm 0.011)\%$, which is in agreement with the measured value of this branching ratio $(0.139 \pm 0.010)\%$.

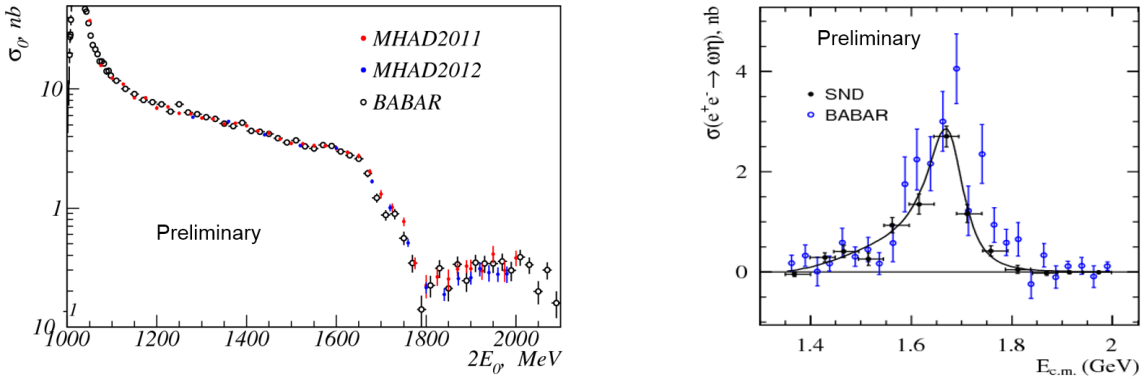


**Figure 3:** The $e^+e^- \to K^+K^-$ (left) and $e^+e^- \to \omega\eta$ (right) cross sections measured by SND in comparison with BABAR data. The solid curve is the result of the VMD fit to the $e^+e^- \to \omega\eta$ data.

In Fig. 3 we show preliminary results on measurement of the $e^+e^- \to K^+K^-$ and $e^+e^- \to \omega\eta$ cross sections. Our results are in reasonable agreement with previous BABAR measurements. The $e^+e^- \to \omega\eta$ is fitted with the VMD model, which includes contributions of the $\omega(1420)$, $\omega(1650)$, and $\phi(1680)$ resonances.

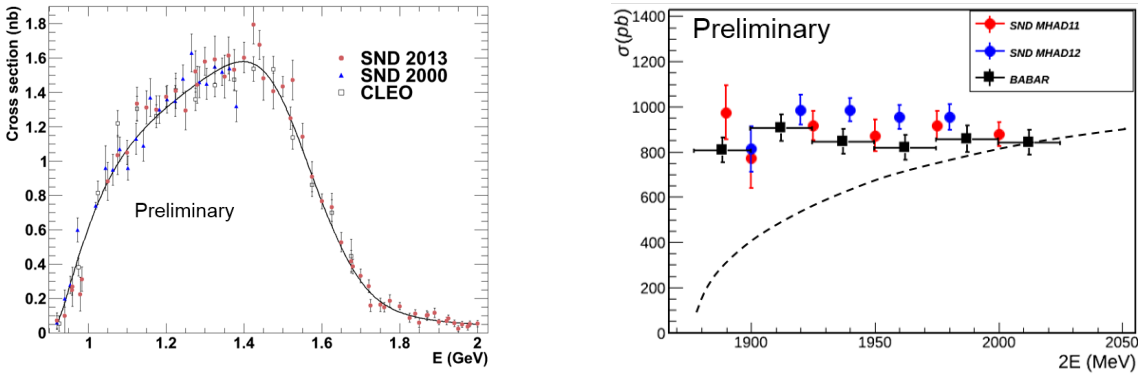


**Figure 4:** Left: The $e^+e^- \to \omega\pi^0 \to \pi^0\pi^0\gamma$ cross section measured by SND at VEPP-2000 (SND 2013) in comparison with the SND data obtained at VEPP-2M (SND 2000) and the data obtained from the spectral function of the $\tau^- \to \omega\pi^-\nu_\tau$ decay measured in the CLEO experiment. The curve is the result of the VMD fit to SND 2013 and SND 2000 data. Right: The $e^+e^- \to p\bar{p}$ cross section measured by SND in comparison with BABAR data.

The update of our measurement of the $e^+e^- \to \omega\pi^0$ cross section [10] based on the full 2010-2013 data set is presented in Fig. 4(left). A mistake in radiative correction calculation, which led to underestimate of the cross section above 1.75 GeV, has been fixed in this new analysis.

## 3. Nucleon production

Our preliminary results on measurement of the $e^+e^- \to p\bar{p}$ cross section is shown in Fig. 4(right) in comparison with BABAR data. The SND and BABAR measurements are in good agreement. It should be noted that the cross section in the energy region under study is close to be constant. Through it is natural to expect its decrease as $\beta = (1-4m_p^2/s)^{1/2}$ when approaching threshold. The proton angular distribution has been also studied. The average over the energy interval under study ratio of the electric and magnetic form factors has been extracted to be $|G_E/G_M| = 1.64 \pm 0.26$. We have confirm the BABAR result, that $|G_E/G_M|$ near threshold strongly differs from unity. It should be noted that $G_E = G_M$ at threshold.

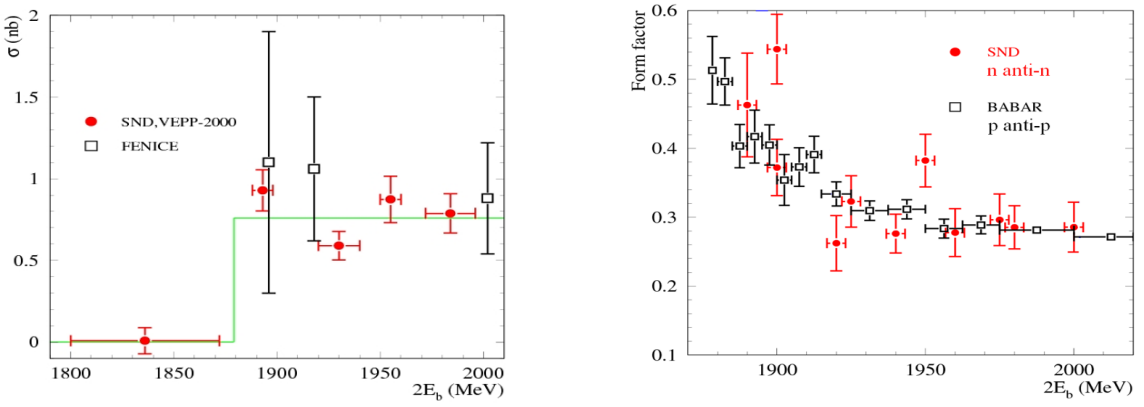


**Figure 5:** Left: The $e^+e^- \to n\bar{n}$ cross section measured by SND and in the FENICE experiment. Only statistical uncertainties are shown for the SND data. Their systematic uncertainty is 17%. Right: The comparison of the proton and neutron effective electromagnetic form factors measured by BABAR and SND, respectively.

Our result on the $e^+e^- \to n\bar{n}$ cross section [11] is shown in Fig. 5(left). The accuracy of the cross section measurement has been significantly improved compared with the only previous FENICE measurement. The $e^+e^- \to n\bar{n}$ cross section is constant below 2 GeV and coincides within the errors with the $e^+e^- \to p\bar{p}$ cross section. Since the proton an neutron cross sections are close, we conclude that either isoscalar or isovector amplitude dominates in the processes of nucleon production near threshold. The comparison of the proton and neutron effective electromagnetic form factors [12] measured by BABAR and SND, respectively, is shown in Fig. 5(right). The growth of the form factors near threshold is explained by the final state interaction [13] or existence of a subthreshold resonance.

## 4. Search for $\eta' \to e^+e^-$ decay

The rare decay $\eta' \to e^+e^-$ is predicted to have a branching fraction of $(1-2)\times 10^{-10}$. Its value is sensitive to the $\eta'\gamma^*\gamma^*$ transition form factor. The strictest limit on the decay branching fraction $B(\eta' \to e^+e^-) < 1.2\times 10^{-8}$ at 90% C.L. was set in 2014 by CMD-3 at VEPP-2000 [14]. Similar to CMD-3, we search for the decay using the inverse reaction $e^+e^- \to \eta'$ [15]. The data with an integrated luminosity of 2.9 fb$^{-1}$ accumulated at the c.m. energy of $957.78 \pm 0.06$ MeV

are used in this analysis. The collider energy spread (FWHM=0.590 MeV) is significantly larger than the $\eta'$ width $\Gamma_{\eta'} = 0.198 \pm 0.009$ MeV. The radiative correction and energy spread leads to reduction of the $e^+e^- \to \eta'$ cross section compared to the Born one by a factor of four. The five decay chains, $\eta' \to \eta\pi^+\pi^-$ with $\eta \to \gamma\gamma$ and $3\pi^0$, and $\eta' \to \eta\pi^0\pi^0$ with $\eta \to \gamma\gamma$, $3\pi^0$, and $\pi^+\pi^-\pi^0$, is used to select $\eta'$ candidates. In these decay modes, no $\eta'$ events have been observed in data. The upper limit has been obtained to be $B(\eta' \to e^+e^-) < 1.0 \times 10^{-8}$ at 90% C.L. The combined SND+CMD-3 limit is $B(\eta' \to e^+e^-) < 5.6 \times 10^{-9}$ at 90% C.L.

We also plan to use the reaction $e^+e^- \to \eta$ to measure the $\eta$ electronic width [16]. The VEPP-2000 parameters at $E = m_\eta c^2 \approx 550$ MeV are following. The luminosity is $0.34 \times 10^{30}$ cm$^{-2}$s$^{-1}$, the accuracy of the energy setting is 60 keV, and the energy spread is $\sigma_E = 150$ keV. The latter may be compared with the $\eta$ full width $\Gamma_\eta = 1.31 \pm 0.05$ keV. We have analyzed a data sample with an integrated luminosity of 108 fb$^{-1}$ collected at $E = 520 - 580$ MeV and found no background events for the reaction $e^+e^- \to \eta$ in the decay mode $\eta \to 3\pi^0$. In absence of background, a sensitivity to $B(\eta \to e^+e^-)$ of $10^{-6}$ can be reached during two weeks of VEPP-2000 operation. Such a sensitivity is better than the current upper limit [17] by a factor of 2.3.

## References


[1] M. N. Achasov *et al.*, Nucl. Instrum. Methods Phys. Res., Sect. A **598**, 31 (2009).

[2] V. M. Aulchenko *et al.*, Nucl. Instrum. Methods Phys. Res., Sect. A **598**, 102 (2009).

[3] A. Yu. Barnyakov *et al.*, Nucl. Instrum. Methods Phys. Res., Sect. A **598**, 163 (2009).

[4] V. M. Aulchenko *et al.*, Nucl. Instrum. Methods Phys. Res., Sect. A **598**, 340 (2009).

[5] A. Romanov *et al.*, in *Proceedings of PAC 2013, Pasadena, CA USA*, p.14.

[6] M. N. Achasov *et al.*, (SND Collaboration), JETP **121**, 27 (2015).

[7] M. N. Achasov *et al.* (SND Collaboration), Phys. Rev. D **91**, 052013 (2015).

[8] S. Godfrey and N. Isgur, Phys. Rev. D **32**, 189 (1985).

[9] A. Donnachie and Yu.S. Kalashnikova, Phys. Rev. D **60**, 114011 (1999).

[10] M. N. Achasov *et al.* (SND Collaboration), Phys. Rev. D **88**, 054013 (2013).

[11] M. N. Achasov *et al.* (SND Collaboration), Phys. Rev. D **90**, 112007 (2014).

[12] The effective form factor is defined as $F(s)^2 = \left[2\tau|G_M(s)|^2 + |G_E(s)|^2\right]/(2\tau+1)$, where $\tau = s/4m_N^2$.

[13] V. F. Dmitriev, A. I. Milstein, and S. G. Salnikov, Phys. Atom. Nucl. **77**, 1173 (2014).

[14] R. R. Akhmetshin *et al.* (CMD-3 Collaboration), Phys. Lett. B **740**, 273 (2015).

[15] M. N. Achasov *et al.* (SND Collaboration), Phys. Rev. D **91**, 092010 (2015).

[16] M. N. Achasov *et al.* (SND Collaboration), JETP Letters **102**, 297 [arXiv:1507.02073].

[17] G. Agakishiev *et al.* (HADES Collaboration), Phys. Lett. B **731**, 265 (2014).